Journal Pre-proof

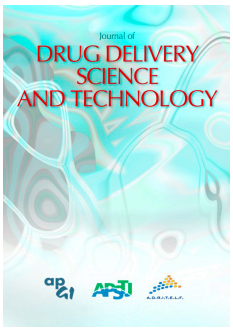

Facile preparation and characterization of injectable self-antibacterial gelatin/ carrageenan/bacterial cellulose hydrogel scaffolds for wound healing application

Fahanwi Asabuwa Ngwabebhoh, Rahul Patwa, Oyunchimeg Zandraa, Nabanita Saha, Petr Saha

PII: S1773-2247(21)00095-2

DOI: https://doi.org/10.1016/j.jddst.2021.102415

Reference: JDDST 102415

To appear in: *Journal of Drug Delivery Science and Technology*

Received Date: 24 November 2020

Revised Date: 5 February 2021

Accepted Date: 5 February 2021

Please cite this article as: F.A. Ngwabebhoh, R. Patwa, O. Zandraa, N. Saha, P. Saha, Facile preparation and characterization of injectable self-antibacterial gelatin/carrageenan/bacterial cellulose hydrogel scaffolds for wound healing application, *Journal of Drug Delivery Science and Technology*, https://doi.org/10.1016/j.jddst.2021.102415.

Author contributions:

This study conceptualization and methodology was performed by Fahanwi Asabuwa Ngwabebhoh. Formal analysis was done by Fahanwi Asabuwa Ngwabebhoh, Rahul Patwa and Oyunchimeg Zandraa. Investigation and data curation were carried out by Fahanwi Asabuwa Ngwabebhoh, Rahul Patwa and Oyunchimeg Zandraa. Writing-original draft preparation was done by Fahanwi Asabuwa Ngwabebhoh. The paper was reviewed, edited and supervised by Nabanita Saha and Petr Saha.

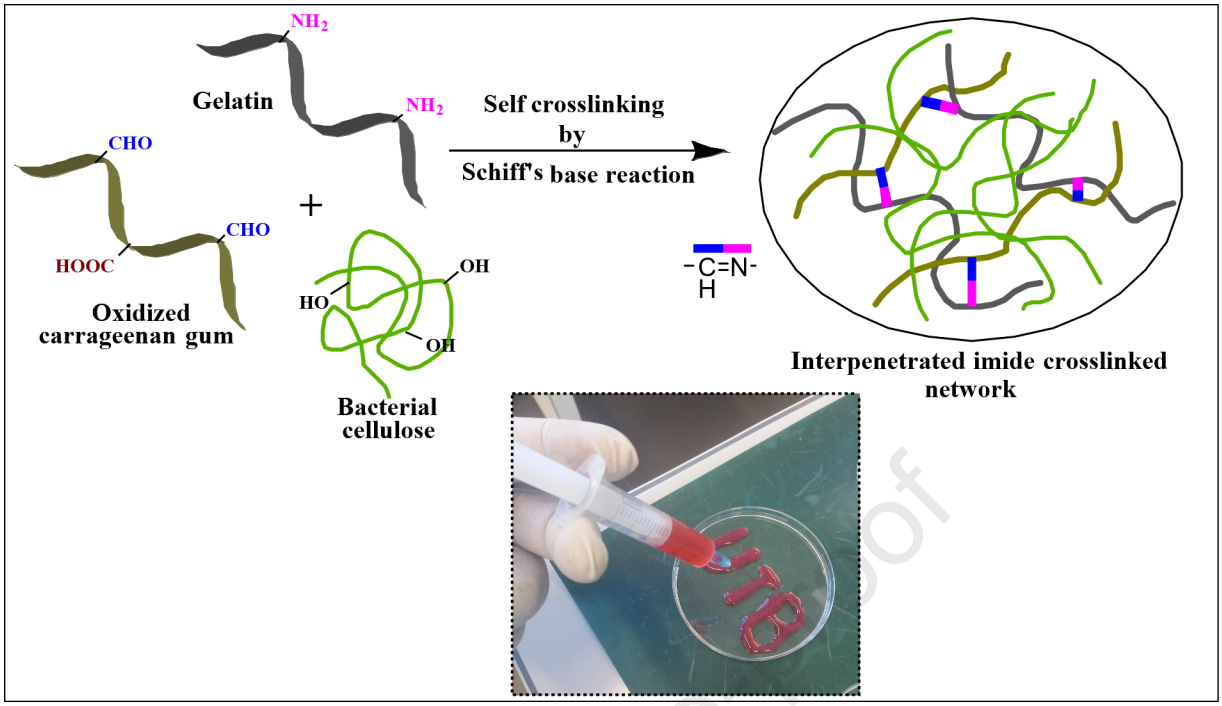

Research Paper

Facile preparation and characterization of injectable self-antibacterial gelatin/carrageenan/bacterial cellulose hydrogel scaffolds for wound healing application

Fahanwi Asabuwa Ngwabebhoh[1,2]*, Rahul Patwa[1,2], Oyunchimeg Zandraa[1,2], Nabanita Saha[1,2,3]*, Petr Saha[1,2,3]

[1]*Centre of Polymer Systems, University Institute, Tomas Bata University in Zlin, Tr. T. Bati 5678, 76001, Zlin, Czech Republic*

[2]*Footwear Research Centre, University Institute, Tomas Bata University in Zlin, Nad Ovcirnou IV, 3685, Zlin, Czech Republic*

[3]*Faculty of Technology, Tomas Bata University in Zlin, Vavrečkova 275, 76001 Zlin, Czech Republic*

Abstract

This study reports the preparation of self-crosslinked Schiff base gels using gelatin and oxidized carrageenan gum interpenetrated with bacterial cellulose (BC) as injectable drug delivery systems. The injectable gels were successfully prepared at body temperature upon blending with BC and loaded with bovine serum albumin (as the model drug) to produce scaffolds. The gel scaffolds were characterized via rheological, FTIR, SEM, XRD, TGA and mechanical compression analysis. Gelation kinetics of gels as well as swelling, *in vitro* degradation and drug release kinetics of gel scaffolds were examined. Results showed that the incorporation of BC to the gel system considerably improved mechanical integrity with remarkable rheological shear-thinning properties. Maximum *in vitro* cumulative drug release from gel scaffolds was determined as 84.01 ± 3.66% within the studied time interval of 168 h. Further analysis showed that the prepared gel scaffolds possess self-antibacterial properties with growth inhibition capacity against *E. coli*, *S. aureus*, and *K. pneumonia*. *In vitro* cell cytotoxicity was also performed by MTT assay and results depicted >80% cell viability, which indicates the gel scaffolds are cytocompatible. In conclusion, this paper presents a facile approach to fabricate all-natural crosslinked injectable self-antibacterial gels systems with prospective potential application in wound dressing and tissue regeneration.

Keywords: Hydrogel, Gelatin, Bacterial cellulose, Drug delivery, Antibacterial activity

Corresponding authors:
E-mail address: F.A. Ngwabebhoh (asabuwa@utb.cz/asabuwa.nf@gmail.com)
N. Saha (nabanita@utb.cz)

1. Introduction

Wound healing as a complex and coordinated process which has been studied extensively towards enhancing healing by using beneficial wound dressing materials. Recently, different wound dressing materials, such as films, nanoparticles, hydrocolloids, and hydrogels have been commercialized and are studied extensively [1, 2]. These dressing materials help provide a moist environment for cell regeneration, protect the wounds from bacterial infections and absorb excess exudate [3]. Amongst these materials, hydrogels have proven attractive features by acting as a physical barrier, fluid absorbent and provide moist scaffold for tissue regeneration. However, most hydrogels have demonstrated to possess low mechanical stability and may require a secondary dressing to adhere on skin tissue [4, 5].

Injectable hydrogels have demonstrated to be attractive wound dressing material as they are less invasive, and can be used for the local delivery of therapeutic agents and cost-effective as it can replace surgical procedures [6]. Over the years, several injectable hydrogels have been developed using synthetic polymers such as poly(N-isopropyl acrylamide), but of which many are non-biodegradable and may lead to local inflammation at infected sites [7]. Naturally-derived polymers or polysaccharides provide the required friendly extracellular matrix for cell attachment and proliferation, which serve as suitable drug carriers and tissue regeneration scaffolds [8, 9]. Gelatin a collagen-derived polymer is made up of peptide sequences that aid in the recognition of integrin receptors in cells, which are vital for cell adhesion in wound healing. However, pristine gelatin possesses low gelling temperature (< 30 °C) that hinders its usage at human body temperature (37 °C) [10]. Therefore, procedures including physical blending and chemical modification have been developed to enhance its gelling conditions. This includes chemical grafting with thiol and methacryloyl groups, use of crosslinking agents such as glutaraldehyde, epichlorohydrin, genipin, or aldehyde-oxidized molecules as well as blending with other polymers to form gels [11-14]. Amongst all, the use of aldehyde-oxidized polymers to form hydrogels via self-crosslinking mechanisms have demonstrated to be very efficient since the toxicity effect of some crosslinking agents are avoided, which to some extent greatly enhances the performance of the hydrogels formed. So far, polysaccharide aldehyde-oxidized moieties have been widely synthesized via oxidation at C2 and C3 position to form excellent polymeric dialdehyde crosslinkers [15]. Carrageenan gum (CG) a linear sulphated polysaccharide mainly extracted from red seaweeds has been widely modified via oxidation using different oxidizing agents such as sodium periodate, sodium hypochlorite, 2,2,6,6-

tetramethylpyperidine-1-oxy (TEMPO) and hydrogen peroxide to produce a biocompatible dialdehyde polysaccharide crosslinker [16-19]. Amongst all, hydrogen peroxide has proven to be the most environmentally friendly since it inevitably decomposes to oxygen and water at the end of the oxidation reaction with no harmful by-product [20]. Therefore, hydrogen peroxide was applied in the present study as the oxidizing agent in the preparation of oxidized CG.

In recent years, the potential of interpenetrating chemically crosslinked hydrogel systems with biopolymeric fibres have attracted great research since this bestows the resultant material with good mechanical integrity [21, 22]. Bacterial cellulose (BC) a linear biopolymer composed of β-1,4-glucopyranose residues commonly biosynthesized using *Komagataeibacter xylinus* bacteria has been use for this purpose [23]. Compared to cellulose extracted from plants, BC shows superior physical and mechanical properties (such as higher degree of purity, high water holding capacity, hydrophilicity and tensile strength) [24]. In addition, BC is highly attractive for biomedical applications due to its non-toxic and biocompatible properties [25]. For example, in wound dressing BC has proven promising due to its complex three-dimensional structure that assures high tensile strength and flexibility providing an adequate moist and thermal environment, which ensures gas and liquid permeability [26, 27].

The choice of polymers and crosslinkage in the development of gels systems for application particularly in the area of wound dressing/tissue regeneration is of utmost importance. In recent years, polymers and gels systems with minimal toxicity to mammalian cells and self-activity against microbes have received considerable attention [6, 28, 29]. Herein, we report the preparation of injectable gels with self-antibacterial properties formed from the crosslinking of gelatin and aldehyde modified carrageenan gum and semi-interpenetration with BC. To the best of our knowledge, this is the first work on such crosslinked injectable gel system with self-antibacterial properties. A gelling mechanism was proposed and the gelation kinetics of the prepared gels investigated. The rheological shear-thinning and self-recovering capabilities as well compression modulus of elasticity of the prepared gels were analysed. In addition, various characterizations were performed for the obtained gel scaffolds as well as swelling and *in vitro* degradation were examined. Cumulative release profile based on the release of bovine serum albumin (BSA) as the model protein drug from the gel scaffold matrix was further evaluated. Also, biological performance

was tested using mouse embryonic fibroblast cells. Finally, antibacterial properties against *E. coli*, *S. aureus*, and *K. pneumonia* were examined.

2. Materials and methods

2.1. Materials

Gelatin powder (Type A, from porcine skin) and kappa-carrageenan gum (CG) were purchased from Sigma-Aldrich. Bacterial cellulose (BC) used was synthesized in our laboratory as described previously [30]. 30 wt% hydrogen peroxide (H_2O_2) was purchased from Pentachemicals Ltd and used as the oxidizing agent. Reagents such as ethylene glycol, sodium hydroxide (NaOH), copper sulphate pentahydrate ($CuSO_4.5H_2O$), calcium acetate $Ca(CH_3COO)_2$, phenolphthalein, and sulphuric acid (H_2SO_4, ≥95% purity) were supplied by Sigma Aldrich. Lyophilized powder of lysozyme (from chicken egg white, protein ≥90%) and bovine serum albumin (BSA, used as the model drug) were also purchased from Sigma Aldrich. All chemicals were used without further purification. Double distilled water was use for the preparation of all aqueous solutions.

2.2. Synthesis of dialdehyde carrageenan gum polymer

The oxidized carrageenan gum (OCG) was prepared via a H_2O_2 and $CuSO_4$ redox reaction as described previously [31, 32]. Initially, 4 g of CG polymer was dissolved in 200 mL of distilled water at 80 °C, followed by cooling to 50 °C. Into the cooled dissolved mixture, 65 mL of 30 wt% H_2O_2 and 10 mL of 0.05 wt% $CuSO_4$, changing the colour of mixture to light brown. The mixture was then reacted at 50 °C for 5 h under constant stirring, which resulted in a colourless solution. The obtained mixture was dialyzed for 3 days using a dialysis bag (molecular weight cut-off 12kDa) to eliminate the copper ions and unreacted H_2O_2. The obtained OCG was subsequently freeze dried and stored until further use.

2.3. Determination of aldehyde and carboxyl content

The aldehyde group content of the prepared OCG was determined via UV absorption method as previously described [33]. OCG was reacted with hydroxylamine hydrochloride and the maximum UV absorbance can be determined at 233 nm using a UV-Vis single beam spectrophotometer (Model I-290), attributed to the formation of π-π conjugation in the molecular structure of converted OCG to oxime via a Schiff's base reaction. The calibration curve was subsequently established using different volumes of 4.22×10^{-4} M glyoxal solution. 2 mL of 1.5% (w/w) $Ca(CH_3COO)_2$ and 2 mL of 0.2% (w/w) hydroxylamine

hydrochloride were added into the different volumes of glyoxal solutions. The mixtures were reacted at 50 °C for 20 min and then cooled. The obtained mixtures were diluted with 50 mL distilled water and measured at 233 nm absorbance. 10 mg of OCG samples were dissolved in 10 mL of distilled water and the determination of aldehyde content was analysed following the procedure described above. The absorbance calibration curve was established and the aldehyde content calculated using the equation: y = 7488.8x + 0.0065 (where, x is the aldehyde content and y is the UV absorbance).

$$\%CHO = \frac{(y - 0.0065) \times 0.05 \times 29}{M \times 7488.8} \times 100 \quad (1)$$

Where, *M* is the dry weight (g) of OCG and 29 is the molecular weight of the aldehyde group. All tests were performed in triplicates and the average values recorded.

The determination of the carboxyl content was performed according to previous reported calcium-acetate consumption method with slight moderations [31, 34]. In essence, carboxyl groups can react with the salts of weak acids such as calcium acetate, forming a carboxyl salt and releasing a same amount of weak acid. Accordingly, 0.045 g of OCG was dissolved in 30 mL of distilled water. 10 mL of prepared 0.1 M $Ca(CH_3COO)_2$ was added and the mixture stirred for 1h to ensure complete reaction between OCG and $Ca(CH_3COO)_2$. The mixture solution was then titrated against 0.01M NaOH from colourless to a stable pink colour using 0.2 %w/v phenolphthalein as the indicator. A control sample analysis was conducted using non-oxidized CG. The percentage of carboxyl groups in the OCG sample was calculated following the equation below:

$$\%COOH = \frac{(V_{OX} - V_C) \times C_{NaOH} \times 45}{W} \times 100 \quad (2)$$

Where, *Vox* and *Vc* are the volumes (L) of NaOH used for oxidized and control sample titrations, respectively. C_{NaOH} is the concentration (M) of prepared NaOH solution, *W* (g) is the weight of sample and 45 is the molecular weight of carboxyl group. Readings were performed in triplicates and the average value recorded.

2.4. Preparation of gels

The compositions of the different gels prepared are presented in Table 1. Firstly, 7 %w/v gelatin stock solution was prepared by complete dissolution in phosphate buffer saline (PBS)

pH 7.4 solution at 80 °C for 30 min. The solution was cooled to 60 °C and under gentle stirring, varying amounts of OCG was added. The mixture was continuous stirred and the pH adjusted in the range 5 to 5.5, in order to promote the reaction between aldehyde and amine functional groups. Subsequently, wet bacterial cellulose was added to the reaction mixture in different weight ratios. Finally, the homogenous mixtures were transferred into petri dishes and allowed to cool to room temperature forming gels samples without BC (GC1 and GC2) and samples interpenetrated with BC (GCB1, GCB2 and GCB3). The formed solid gel samples were then washed multiple times with distilled water to remove unreacted components and freeze dried to form gel scaffolds. The prepared gels and freeze-dried scaffolds were stored and used for further analyses.

Table 1
Compositions of the all-natural prepared gels.

Sample	Gelatin (%w/v)	OCG (%w/v)	BC (%w/w)
GC1	7	0.5	/
GC2	7	1	/
GCB1	7	1	0.5
GCB2	7	1	1
GCB3	7	1	2

2.5. Gelation kinetics and swelling analysis

In this study, gelation as a function of time was evaluated via the inverted tube test method as described previously with slight moderation [35, 36]. In brief, 1 mL of the different gel solutions prepared as described above were transferred into 1.5 mL vials. The vials were further incubated in a temperature-controlled bath for a period of time. The sol-gel transition time of the gel samples was determined by interval control of the test vials in the bath and inverted every minute. If the test vial containing the solution is titled and a deformation flow occurs, is defined as a sol phase, while if no flow occurs it is described as a gel phase. The time at which the gel did not flow was recorded as the gelation time.

The equilibrium swelling capacities of the prepared gels was measured by immersing the freeze-dried weighted samples in PBS (pH 7.4) at 37 °C and at different time intervals of 6, 12 and 24h, the samples were extracted, blotted with tissue paper to remove excess water and weighed. Readings were performed in triplicate and the average swollen value recorded. The equilibrium swelling percentages (ES%) were calculated using the equation below:

$$ES\% = \frac{W_t - W_i}{W_i} \times 100 \qquad (3)$$

Where, W_t is the weight of the swollen gels after 24h and W_i is the initial weight of the freeze-dried gels.

2.6. Viscoelastic and mechanical properties of gels

Rheological measurements were conducted on a rotational rheometer (Anton Paar MCR 502) with parallel plate geometry of 25 mm diameter. Initially, an amplitude sweep measurement was conducted to determine the linear viscoelastic range (LVE) for the gels. Next, storage modulus (G′) and loss modulus (G″) were measured as a function of change in temperature from 18 to 50 °C at a fixed heating/cooling rate of 2 °C/min and constant frequency of 1 Hz in the LVE of 1% of strain. Finally, strain sweep studies were performed by varying the amplitude from 0.01 to 100% at constant frequency of 1 Hz. Two replicate measurements of each gel sample were performed and the average value of the obtained results over time was determined. The compression modulus of elasticity of the gels was evaluated by unconfined compression at 25 °C using a Testometric MT350-5CT (Labomachine, Czech Republic). Prior to analysis, the formed solid gels were severally washed with distilled water and cut into cylindrical shapes. The compressive modulus was then measured under a static load of 5 kg and crosshead speed of 1 mm/min.

2.7. Characterization of gel scaffolds

Fourier transform infrared (FTIR) spectra of the pristine polymers and gel scaffold samples were recorded using a Nicolet iS5 (Thermo Scientific, USA), scanned at a resolution of 4.0 cm^{-1} in the range of 4000−400 cm^{-1}. The surface morphology of the gel scaffolds was observed by scanning electron microscopy (SEM) using a bench-top Phenom™ Pro microscope operating at 10 kV. The crystallinity of the samples was analysed by a high-resolution Mini Flex™ 600 X-ray diffractometer (Rigaku, Japan). The scans were conducted in the range of 0 - 90 °, at a speed of 5 °/min using a Cobalt radiation at 40 kV and 15 mA. Thermogravimetric analysis (TGA) was conducted using a Q500 thermogravimetric analyser at a heating rate of 10 °C/min from 25 to 600 °C under a nitrogen flow rate of 40 - 60 mL/min.

2.8. Drug loading efficiency, drug release and kinetics study

BSA was used as the model protein for drug delivery investigation. The initial loading concentration of BSA in the gels was 5 mg/mL. Briefly, BSA was incorporated into the gels by first heating the gel mixture to 60 °C, followed by cooling to ≈40 °C, and then loading of

BSA into the gel systems added under gentle stirring. The gel solutions were allowed to stir for 2h and further cooled down to room temperature to obtain solid BSA-loaded gels. The loaded samples were then freeze dried and the obtained scaffolds used for further analysis. In order to calculate the drug loading efficiency, the BSA-loaded gel scaffolds were weighed, immersed in PBS and crushed to release the drug. The mixture was centrifuged at 14000 rpm, the supernatant collected and the absorbance determined at 280 nm (corresponding to the absorbance of tyrosine and tryptophan) using a UV-VIS single beam spectrophotometer (Model I-290). Using a standard calibration curve of BSA in PBS, the drug loading efficiency percentage (DLE%) was calculated according to the equation below:

$$\text{DLE\%} = \frac{Total\ amount\ of\ BSA\ added - \ Amount\ of\ BSA\ in\ supernatant}{Total\ amount\ of\ BSA\ added} \times 100 \quad (4)$$

The *in vitro* release study was conducted according to previous reported procedures with slight modification [37, 38]. In brief, BSA release from the prepared hydrogels was studied in PBS of pH 7.4 using a shaking water bath (100 rpm) at 37 °C. BSA-loaded hydrogels were immersed in 100 mL of PBS solution and placed in the water bath for release. At predetermined time intervals, 1 mL of release medium was collected and the amount of BSA analysed spectrophotometrically using a UV-VIS single beam spectrophotometer (Model I-290) at 280 nm. In order to maintain a constant release medium volume, the collected sample for analysis was replace with same amount of fresh PBS solution. The amounts of released BSA were determined from the calibration curve and the cumulative drug release percentage (CD%) was calculated according to the equation below:

$$CD\% = \frac{D_t}{D_0} \times 100 \quad (5)$$

Where, D_t is the total amount of BSA released at time *t* and D_o is the initial amount of BSA in the gel scaffolds. In order to establish the mechanism of drug release kinetics, the release data of BSA from the gel scaffolds were computed and fitted to four widely use kinetic models; Zero-order (Eq. 6), First-order (Eq. 7), Higuchi (Eq. 8) and Korsmeyer-Peppas model (Eq. 9) [39-41]. The mathematical expression is provided below:

$$M_t = K_o t \quad (6)$$

$$LnM_t = LnM_o - K_1 t \quad (7)$$

$$M_t = K_H t^{1/2} \quad (8)$$

$$LnM_t = nLnt + LnK_{KP} \quad (9)$$

Where, M_t is the amount of drug released at time *t*, M_o is the initial concentration of drug and the parameters K_o, K_1, K_H and K_{KP} are the rate constants related to the cumulative drug release for Zero-order, First-order, Higuchi, and Korsmeyer-Peppas models. n is an indicator of the drug release mechanism, that is a value of $n \leq 0.5$ indicates that drug release is controlled by Fickian diffusion. A value of $n \geq 1.0$ suggests a non-Fickian diffusion with characteristic of zero-order release rate and values in the range $0.5 < n < 1.0$, indicates that the release process is anomalous. Values of n = 0.5 and 1.0 describes case I and II transport processes, respectively, which are characterized by polymer relaxation related to polymer erosion during enzymatic degradation [42, 43]. Considering Korsmeyer-Peppas model is valid only within the 60% range of the cumulative drug release curve, all studied kinetic models were fitted to the first 60% cumulative release data of the drug release curve [44].

2.9. In vitro cell cytotoxicity, enzymatic degradation and antibacterial analysis of gel scaffolds

To evaluate the cytocompatibility of the prepared gel scaffolds, the samples were cut into 15 mm diameter disks, swollen in culture medium for 2h and the extracts prepared (0.1 mg/mL of culture medium) according to ISO standard 10993-12. ATCC–formulated Dulbecco's Modified Eagle's (DMEM) medium (Biosera, France) containing 10% of calf serum and 100 U/mL penicillin/streptomycin (Biosera, France), was used as the culture medium. The extract was diluted with the culture medium to obtain following concentration: 50, 75 and 100 % of parent extract. All assays were performed in triplicates with the extracts used within 24h. Mouse embryonic fibroblast cells (ECACC 93061524, England) were seeded to pre-incubated microtitration test plate dishes (TPP, Switzerland) at a concentration of $1x10^5$ cells/mL. The sucked-up culture medium was replenished. The cell viability was measured using Tetrazolium (MTT cell proliferation assay kit, Duchefa Biochemie, Netherlands). The absorbance of the solutions was measured spectrophotometrically at 570 nm. The results are presented as reduction of cell viability in relative values when compared to cells cultivated in medium without the extracts of tested samples.

The degradation of the gel scaffolds was investigated with respect to weight loss in PBS pH 7.4 aqueous solution over a period of 14 days. Initially, 0.1 %w/v enzymatic solutions

were prepared by dissolving calculated amounts of lysozyme in PBS. The freeze-dried gel scaffolds were weighed (*Wo*), immersed in the PBS solutions and incubated under mild shaking of 100 rpm in an oven at 37 °C. At specified time intervals, the gel samples were removed from the PBS solution, gently blotted with filter paper, dried and weighed (*Wt*). In order to simulate continuous lysozyme activity, 5 mL of the degradation solution was refreshed every 2 days. Readings were performed in triplicates and the average values recorded. The extent of in vitro degradation was expressed as the percentage weight loss (%WL) using the equation $((Wo - Wt)/Wo) \times 100$.

Antibacterial activity of prepared non-loaded and loaded gel scaffolds was assessed against *Escherichia coli (CCM 4517), Staphylococcus aureus (CCM 4516),* and *Klebsiella pneumonia (CCM 4415)* using the agar disc diffusion test. Typical, 100 µL aliquot of each bacterial stock suspension of approximate concentration 12 x 10^8 cells/mL was uniformly spread on a tryptone soya agar plate and the gel scaffold samples (6 mm diameter) placed on top of the plates. The plates were then incubated at 37 °C for 18h and the inhibition zones measured.

2.10. Statistical analysis

All experimental data were analysed using Analysis of Variance (ANOVA). Statistical significance was evaluated at p-value ≤ 0.05. All results are presented as mean ± standard deviation.

3. Results and discussion

3.1. Gel fabrication and gelation kinetics

Based on the synthesis of OCG from CG in the present study, a possible chemical reaction phase is presented in Fig. 1. In essence, the oxidation of CG was performed using H_2O_2 and $CuSO_4$ as the oxidant and catalyst, respectively [31, 45]. The reaction mechanism occurred via a radical initialized process where in the presence of copper ions, H_2O_2 quickly decomposed to different radicals such as HO•, HO_2•, and O_2•. These generated reactive free radicals rapidly reacted with the hydroxyl groups of CG, resulting in the formation of aldehyde (CHO) and carboxyl (COOH) groups on the backbone chain of CG [46]. The content percentages of CHO and COOH for the final oxidized product was determined as 1.04 ± 0.06 and 11.60 ± 0.03%, respectively. This indicated that CHO and COOH groups were successfully incorporated into CG structure. Subsequently, the preparation of the

injectable gels was carried out by crosslinking gelatin and OCG followed by fibrillar interpenetration with bacterial cellulose (Fig. 1a). The crosslinking process predominantly occurred due to Schiff's base reaction between the free ε-amines (-NH_2) of lysine or hydroxylysine side groups of gelatin and the grafted aldehyde groups of OCG forming imide bonds [47]. By physical visualization, it was observed that the viscosity of the crosslinked mixture between gelatin and OCG gradually increased with time forming weak translucent gels. These weak formed gels were further improved by fibrillar interpenetration with bacterial cellulose (Fig. 1b), which in turn increased the viscosity of the mixture and formed gels with enhanced mechanical stability that could self-support its own weight at 37 °C.

Gelation rates of the different prepared gels were monitored at 37 °C and the time of gel formation determined as 23, 15, 12, 7 and 4 minutes for investigated GC1, GC2, GCB1, GCB2 and GCB3, respectively. As observed, the gelation time of GC gels were longer compared to that of GCB. Gelation time of GC gels occurred between 15 to 25 min as compared to GCBs that was in the range of 4 to 12 min. The fast gelation in GCB gels was attributed to the incorporation of BC. The effect of BC was confirmed as the gelation time gradually decreased with increase in BC ratio. As such, GCB3 with the highest BC content reached complete gelation within 4 min, exhibiting a considerably faster gelation rate than the other gels. It is obvious that the addition of BC in the crosslinked gel systems significantly reduced the gelation time. This fast gelation may be attributed to the increase in total viscosity of the gel mixtures that in turn enhanced intra/intermolecular hydrogen bond interaction, forming a high dense 3D physical and chemical crosslinked network. The images of the formed gels after their gelation times are displayed in Fig. 1c.

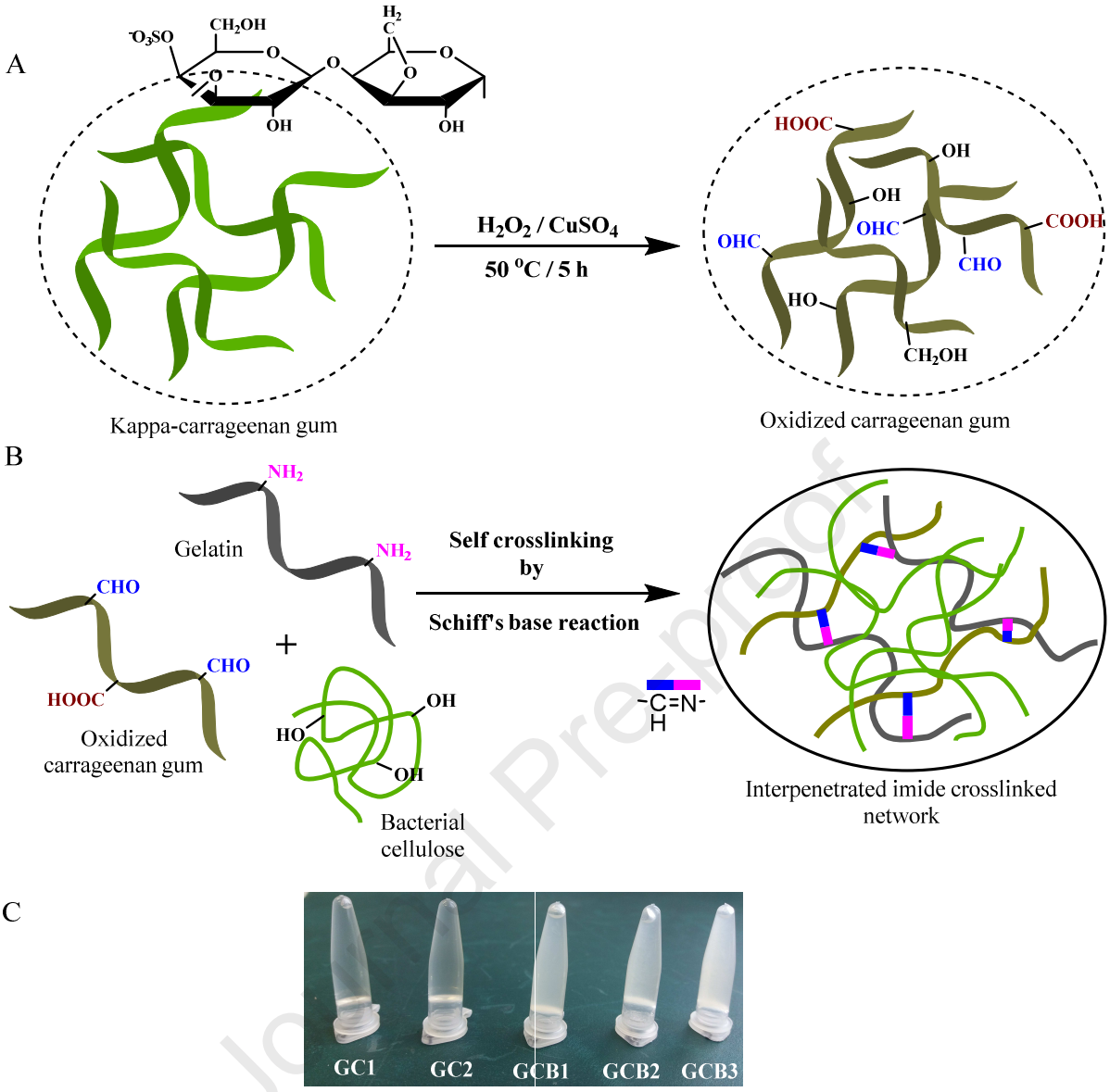

Fig. 1. a) Schematic representation for the synthesis of oxidized carrageenan gum, b) proposed crosslinked network in gels via Schiff base reaction and c) the images of the different formed gels at 37 °C.

3.2. In vitro swelling and degradation analysis of freeze-dried gel scaffolds

Water absorption ability is an important parameter to predict the movement of oxygen and nutrients within a given crosslinked gel structure [48]. Fig. 2a shows the swelling results of the prepared freeze-dried gel scaffolds swollen in dH_2O as a function of time to reach equilibrium water uptake. According to the results obtained, maximum swelling was reach within 12 h for GC gel scaffolds. However, GC1 showed higher swelling when to GC2, which can be attributed to the low crosslink density of GC1. After 24 h, GC gels depicted drastic decrease in swelling capacity and such possible occurrence could be attributed to the gradual dissolution/degradation of the gel structural network considering gelatin is

temperature sensitive. Notwithstanding, an increase in the crosslink density in GC2 showed slower dissolution as compared to GC1. Following the incorporation of BC in the gel systems, higher swelling values were achieved after 24 h. But a decrease in water uptake was observed within the GCB gel scaffolds as BC content increased. The possible reason associated to this relates to the formation of more hydrogen bonds as well as the effect of inter/intramolecular interaction in the gel network as BC amount increased, which in turn restricted the swelling of the gel scaffolds. Overall, the maximum equilibrium swelling values after 24 h were determined as 280.42 ± 19.02, 340.98 ± 11.89, 620.14 ± 30.60, 550.48 ± 27.47 and 460.38 ± 22.86% for GC1, GC2, GCB1, GCB2 and GCB3, respectively.

In vitro biodegradation of the gels and their scaffolds is considered a crucial parameter particularly in wound healing applications. This is because the gel provides mechanical strength support to the wound, protects the wound against infections and aids in the release of loaded bioactive molecules that promote wound healing [28]. In the present study, enzymatic degradation studies were performed to determine the stability of the prepared gel scaffolds. Herein, lysozyme was employed as the degradation enzyme prepared at a concentration of 0.1 %w/v to mimic an *in vivo* degradation system and the weight loss of the gel scaffolds were monitored in PBS at 37 °C within a period of 14 days. Fig. 2b depicts the degradation of GC and GCB gel scaffolds based on weight loss as a function of time. As expected, a faster weight loss was observed for gel scaffolds without BC (GC1 and GC2) compared to samples with BC (GCB1, GCB2 and GCB3). According to observed results, GC1 and GC2 completely degraded in less than 5 days while GCB gel scaffolds showed more than 50% weight loss on the 5^{th} day. On the 5^{th} day of incubation, the weight loss of GCB gel scaffolds was determined as 66.58 ± 3.32%, 60.80 ± 3.04% and 52.29 ± 2.61% for GCB1, GCB2 and GCB3, respectively.

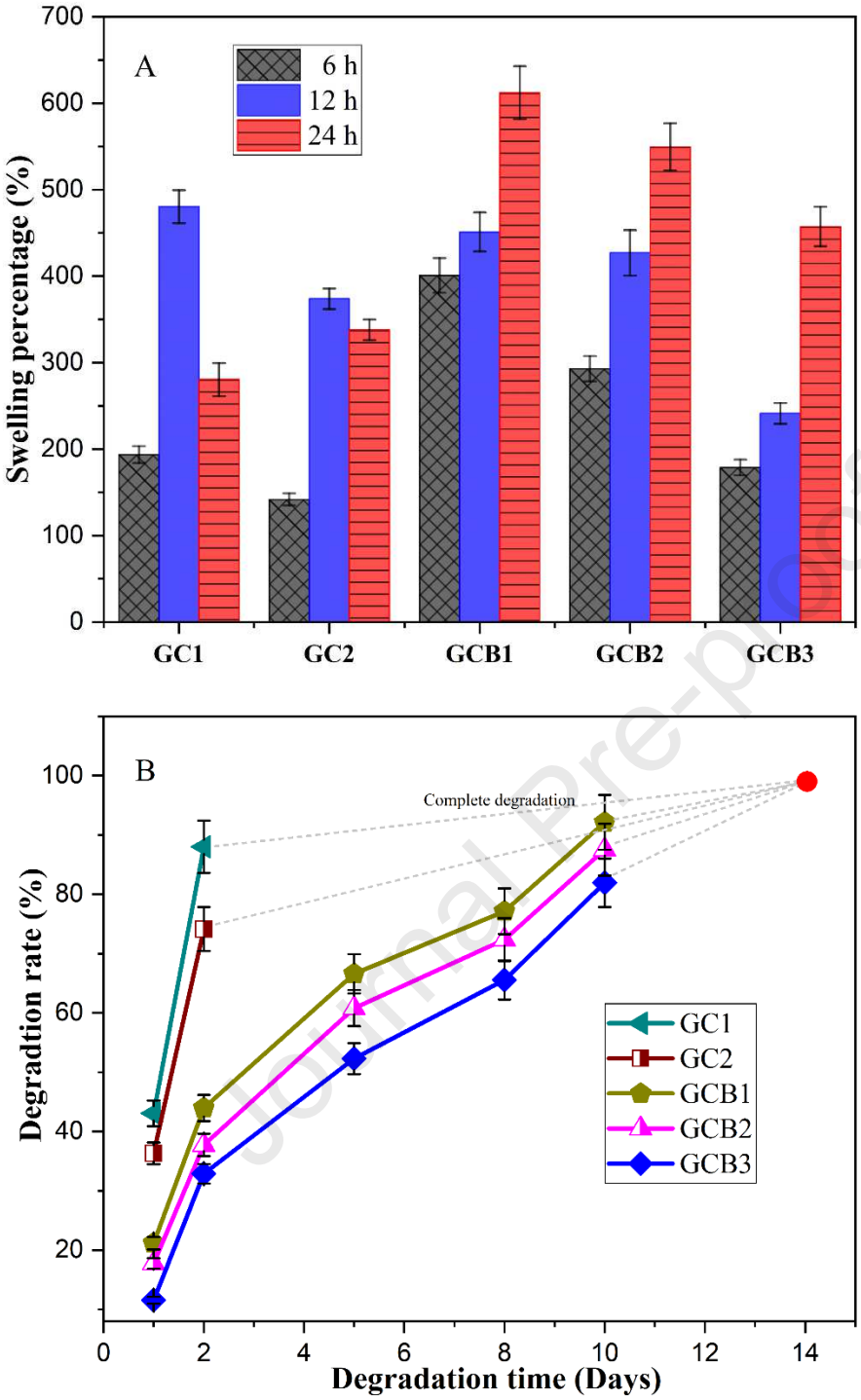

Fig. 2. a) Swelling capacity and b) enzymatic degradation of prepared gel scaffolds as a function of time.

Thus, it is evident that the incorporation of BC increased the stability of GCB gel scaffolds, which in tend decreased degradation rate as compared to GC samples. This gel matrix stability may be attributed to induced fibrillar meshwork structure formation and intra/intermolecular hydrogen bonding introduced by BC that retarded degradation of the GCBs. This contributes to the beneficial properties of this material for application during

wound healing application. Overall, the first 5 days of degradation were mostly attributed to sufficient swelling of the gels in solution and thereafter, the degradation increased due to gradual disintegration of gel structural network via crosslinked sites. GCB gel scaffolds showed >80% weight loss after 10 days with complete degradation within 14 days. Based on the swelling and degradation studies discussed, GC2 (as control) and GCB2 samples were further analysed in the present study and subsequently designated as GC and GCB, respectively.

3.3. Characterization techniques

3.3.1. Rheological and compression properties of prepared gels

The rheological properties of the prepared gels were analysed via oscillatory rheology to demonstrate the stability of the samples after shear deformation. Fig. 3a and b displays the temperature sweep tests of storage modulus G′ and loss modulus G″ within a temperature range of 10 to 50 °C. According to literature [1], gelatin is unable to form gels at body temperature (G′ < G″) but forms gels at lower temperature below 27 °C (G′ > G″). However, by crosslinking gelatin with a small amount of carrageenan gum causes a big difference whereby the obtained gels (GC) show resistance to temperature evolution where G′ is larger than G″ in the range of 10 − 35 °C, indicating the effect of oxidized carrageenan gum in the gelling process of gelatin. By adding BC to the gel matrix to produce GCB, higher G′ values are achieved compared to that of GC gels. This increase in G′ may be attributed to intermolecular complex formation between the chemical crosslinked network and BC via physical crosslinking. At temperature ≥37 °C, G′ of GCB gels was steadily larger than G″, suggesting the network of the gels are less thermosensitive as compared to GC that are less stable. In addition, amplitude sweep studies were performed by subjecting the gels to varying strains ranging from 0.1% to 100%. In conformity to Fig. 3c and d, these gels showed signs of crossover at around strain values of 45 and 58% for GC and GCB gels, respectively. Within 100% strain, the addition of BC led to a higher elasticity, which probably equipped the GCB gels with the more capability to withstand administration-related strains as an injectable formulation. Moreover, the rigidity in chemical structure of some natural polysaccharides such as carrageenan gum, enables them to be use utilized as modifiers for tuning rheological properties thereby endowing the prepared gels with desirable shear-thinning properties [49]. In addition, bacterial cellulose greatly contributed to the shear thinning properties via its fibrillar structures that can re-order in the flow direction of the gels

as they display decrease in viscosity with loss in their network structure [50]. As such, the prepared GCB gels in the present study can be extruded via injection needles forming different patterns (Fig. 3e). The extruded gels quickly reassemble within minutes upon cessation of shear. This result is in accordance with the rheological test and may be attributed to the good shear-thinning properties arising from carrageenan gum and bacterial cellulose that have been widely applied as injectable matrix for tissue regeneration in wound healing application [29, 51].

The mechanical properties of wet GC and GCB hydrogels were determined under compression at 80% strain. Fig. 3f displays the results obtained during the compression process of the gels. From the stress–strain curves and compressive modulus, the incorporation of BC in the crosslinked gel matrix showed great effect on the stress–strain behaviour and compressive modulus of elasticity of the prepared gels. Based on deduced results, the compressive modulus was determined as 6.5 ± 0.35 and 22.3 ± 1.40 kPa for GC and GCB gels, respectively. This indicated that the mechanical properties of the gels were significantly improved due to interpenetration of GC gel matrix with BC [52]. Overall, the addition of BC in the gels greatly enhanced the mechanical stability of the gels making it suitable for application as injectable formulation.

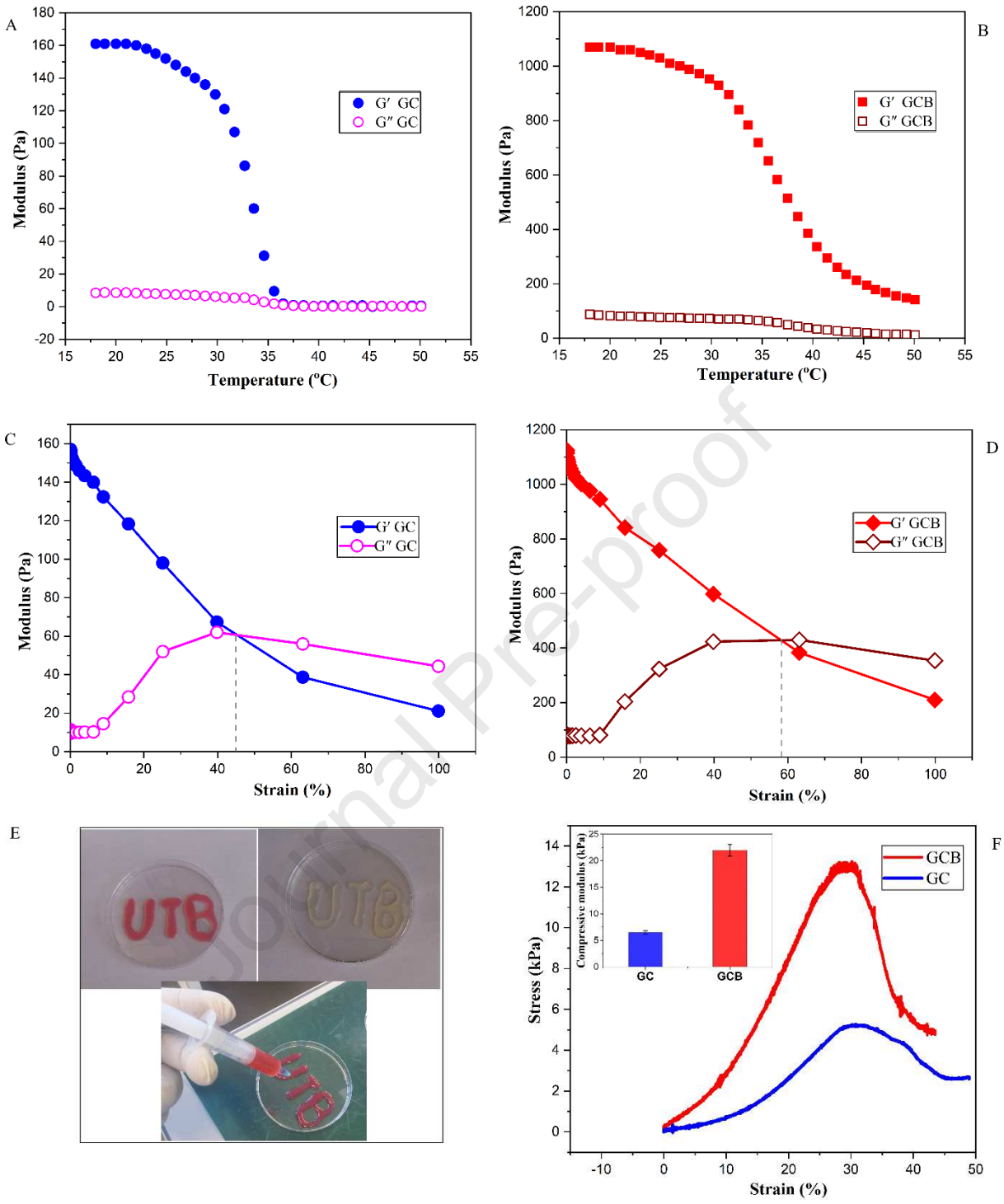

Fig. 3. Rheological measurements of GC (control) and GCB gels a) and b) temperature sweep at constant frequency of 1.0 Hz and strain of 0.1%, c) and d) strain sweep at constant frequency of 1.0 Hz and temperature 25 °C, e) images of dyed and non-dyed GCB gel extruded from a 22-gauge syringe forming different patterns and f) the stress-strain curves and compressive modulus of elasticity of GC and GCB gels at 25 °C.

3.3.2. Analysis of freeze-dried gel scaffolds

The FTIR spectra of the different samples are presented in Fig. 4. According to obtained results, CG and OCG displayed characteristic peaks at around 3426, 2935, 1240, 928 and 840 cm^{-1}. The strong broad band at around 3426 cm^{-1} is attributed to hydroxyl (OH) group stretching. The peak at 2935 cm^{-1} is assigned to the asymmetric stretching vibration of methyl and methylene groups. The peaks at 1240 and 847 cm^{-1} are assigned to the symmetric vibration of $-SO_4$ and C_4—O-S attached on β-D-galactose carrageenan structure, respectively [31]. The peak at 1050 and 928 cm^{-1} relates to the asymmetric stretching vibration of C−O and C−O−C of 3,6-anhydro-D-galactose in CG. By comparing CG and OCG, results suggest that the primary structure of carrageenan gum was not destroyed during oxidation. However, a new characteristic peak appeared around 1734 cm^{-1} in the spectrum of OCG, which is attributed to the stretching vibrations of C=O [53]. This confirms that carboxyl and aldehyde groups were successfully introduced in the backbone structure of CG via selective oxidation. By further analyses of GC and GCB spectra, characteristic peaks of pristine gelatin were observed. This includes the peak at 1734 cm^{-1} that relates to C=O stretching of β-lactam, 1643 cm^{-1} ascribed to both C−O stretching of primary amide and C−C stretching of benzene ring and the peak at 1556 cm^{-1} that describes both N-H in-plane bending and C=N stretching of secondary amide groups in the structure of gelatin [54]. While the broad peak between 3500 and 3200 cm^{-1} corresponds to the overlapped stretching vibrations of N-H from gelatin and OH groups of OCG and BC. In addition, the peak at 1244 and 1050 cm^{-1} are attributed to the C−O asymmetric bridge stretching and C−O−C vibration of OCG and BC. However, the stretching vibrations of the imine group (C=N) formed via Schiff base reaction from the reaction of primary amino groups of gelatin and the aldehyde groups of OCG usually appears around between 1640 to 1520 cm^{-1}, but was overlapped by the strong functional C=N group peaks of pristine gelatin in this region [55].

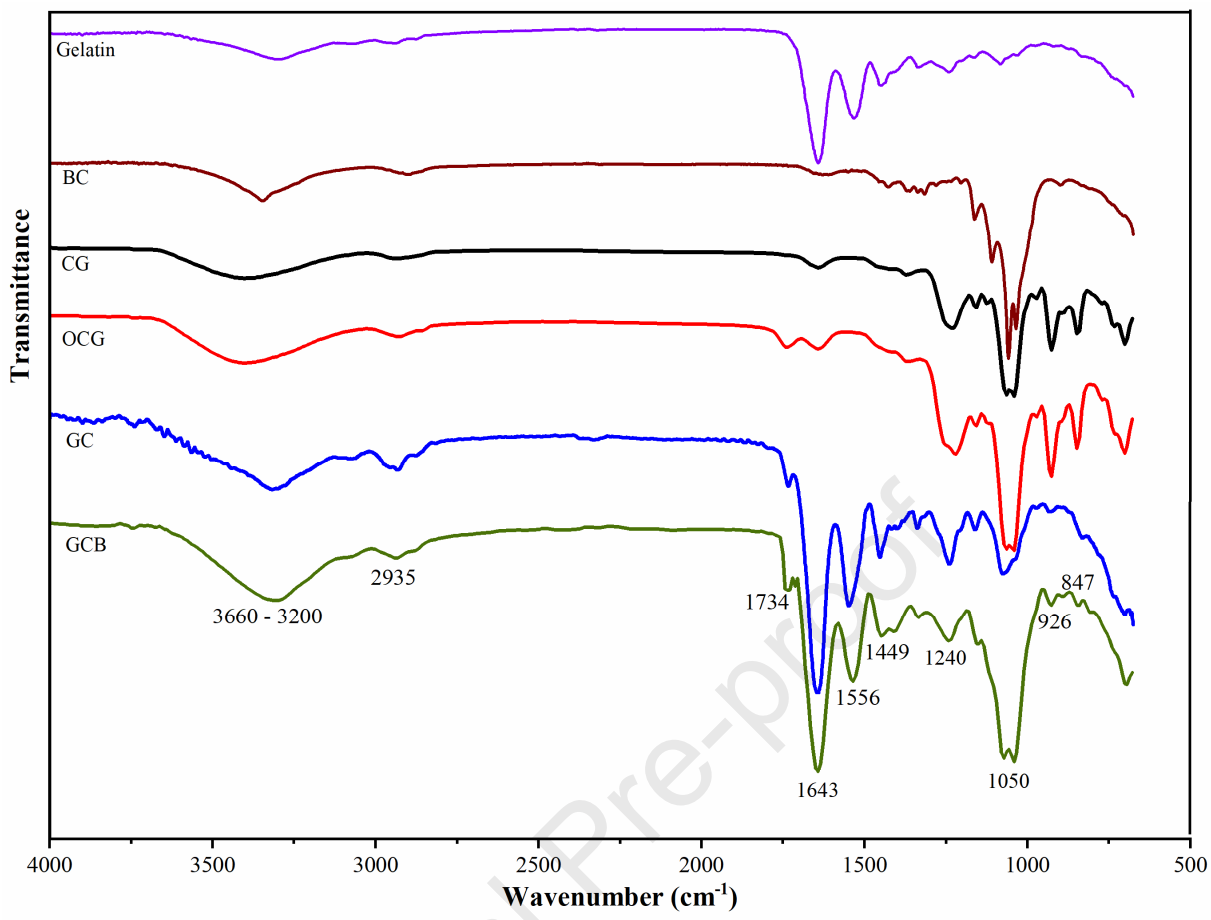

Fig. 4. FTIR spectra of investigated samples.

Fig. 5 displays the X-ray diffractograms Gelatin, BC, GC and GCB. According to literature [56], a polymer matrix with sharper and stronger peaks depicts higher degree of crystallinity, while polymeric systems with relatively weak and wide range peaks shows the presence of amorphous regions. As observed, the diffractograms of the prepared GC and GCB gel scaffolds were mainly dominated by two peaks at 2θ = 9.60° and 21.39° relating to the partial crystallinity characteristic of gelatin. These characteristic peaks are generally assigned to the triple-helical crystalline structure in gelatin [57, 58]. Following the results obtained, GC displayed lower peak intensity of ≈480 counts at 2θ = 21.39° compared to ≈675 counts determined for GCB. This additionally confirms the effect of incorporated BC in the gel structure that in tend increased the degree of crystallinity GCB matrix. Furthermore, the shift of the peaks corresponding to BC in GCB confirms the homogeneous interaction between BC fibrillar mesh network with the crosslinked gel matrix [59].

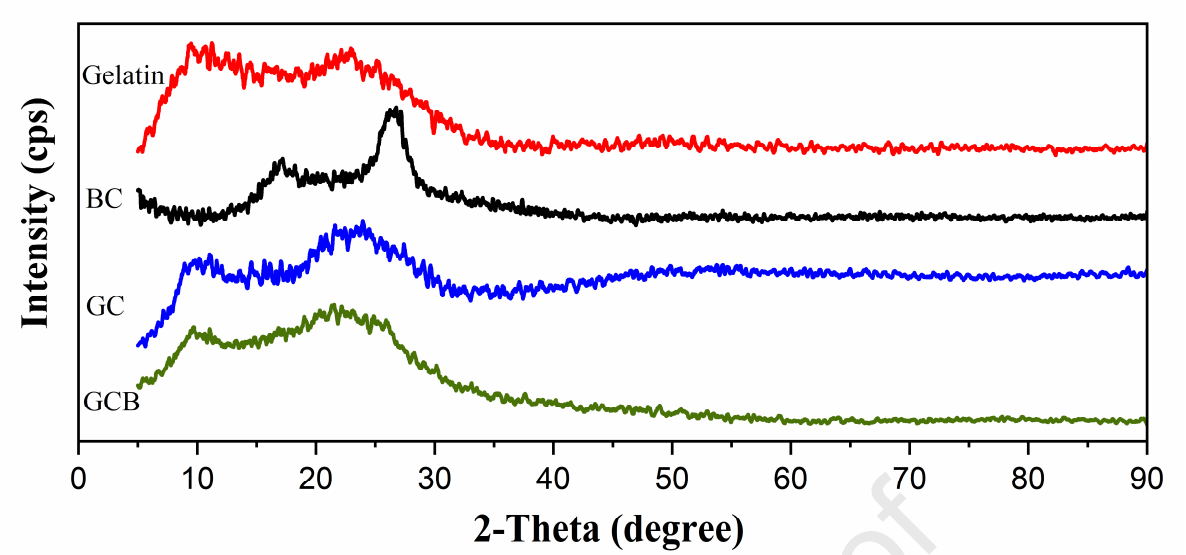

Fig. 5. X-ray diffractograms of gelatin, BC and prepared gel scaffolds (GC and GCB).

The surface morphologies of GC and GCB gel scaffolds were examined and the SEM images are shown in Fig. 6a and b. Both gel scaffolds showed fairly regular, aligned and straight channels with continuous micrometer size honeycomb-like morphology. In conformity, it can be observed that the cross-sectional morphology GC was slightly different from that of GCB. According to the figures, a denser and fibrillar mesh network was displayed by GCB gel scaffolds. This can be attributed to the homogenous interpenetration BC fibrils within the crosslinked GC matrix. Similar results on the preparation microbial cellulose blended gelatin materials has been previously reported by Taokaew et al. [60]. In addition, the prepared GC and GCB gel scaffolds demonstrated to be porous with average pore diameters of 200 μm, which tissue regeneration may favour cell migration and differentiation within the gel scaffolds.

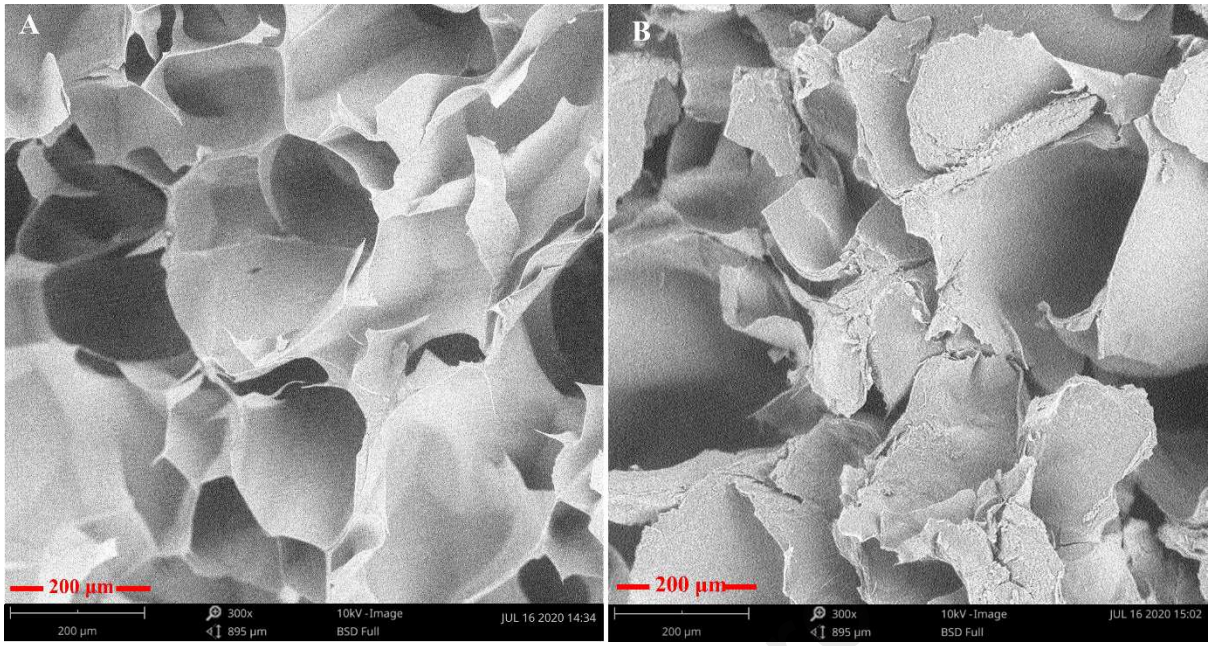

Fig. 6. SEM images of freeze-dried a) GC and b) GCB gel scaffolds.

The thermal behaviour of GC and GCB gel scaffolds is of importance with regards to their stability and controlled drug release mechanism. According to Treesuppharat et al. [61], the thermal behaviour of hydrogels depends majorly on the thermo-responsive capability of their crosslinked network. The TG and DTA curves of GC and GCB gel scaffolds are displayed in Fig. 7. As observed, the variation in weight loss can be classified into three different phases. From 25 to 200 °C, the weight loss was related to evaporation of free water molecules within the gel structure. From 200 to 500 °C, the sharp weight loss was attributed to polymeric chain and crosslinked network degradation. At temperature above 480 °C, relates to the thermal decomposition associated with polymeric backbone leading to the formation of char residue. Thus, it is suggested that the usage of GC and GCB gels for drug-delivery systems is suitable at temperatures below 200 °C.

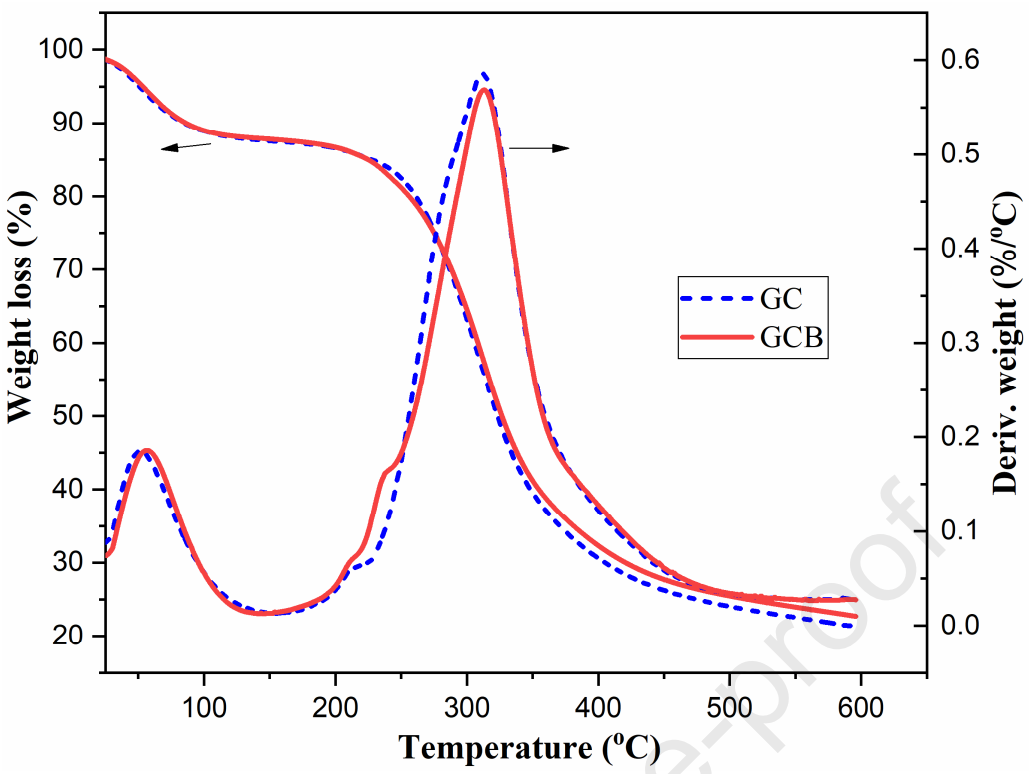

Fig. 7. Thermal degradation behaviour of GC and GCB gel scaffolds.

3.4. In vitro cell cytocompatibility and protein release study of gel scaffolds

Considering the prepared materials are applied as drug delivery vehicles and dressings, the toxicity of gels is investigated. In order to evaluate the cytotoxicity, different extract concentrations (50, 75 and 100%) of GCB (as control) and drug loaded gel scaffolds (BSA-GCB) were seeded with mouse embryonic fibroblast cells and measured by MTT assay. Based on deduce results, cell viability on GCB and BSA-GCB gel scaffolds depicted to be higher than 80% as shown in Fig. 8a. This indicated that GCB scaffolds are cytocompatible with low toxicity. Thus, this confirms the high efficiency of the prepared gel scaffold to promote cell growth and proliferation during tissue regeneration application. In addition, this revealed that the gel scaffold is suitable for maintaining proliferation of cells due to its similar physical structure and chemical composition as that of tissue matrix.

According to Kiortsis et al. [62], controlled release systems consist of a matrix-drug and polymeric assembly that follows a three-step release process; hydration of the drug matrix by release medium, swelling of the polymer matrix leading to disintegration, and lastly the transportation of the dissolved drug for release into the surrounding medium. In the present study, the drug delivery study was evaluated based on the release of BSA from GC (control) and GCB gel scaffolds. According to performed calculations, the drug loading efficiency of

514 BSA in GC and GCB gel scaffolds was determined as 69.2 ± 2.43% and 64.8 ± 1.88%,
515 respectively. Fig. 8b shows the cumulative release of BSA from GC and GCB. As observed,
516 the initial burst release from GC (17.37 ± 1.64%) was approximately twice the release of
517 GCB (9.33 ± 2.01%) gel scaffold. This indicated that a sustain release process was achieved
518 for GCB by the incorporation of BC in the gel matrix. Based on the investigated release time
519 interval, cumulative drug release of 43.85 ± 3.24% and 31.53 ± 1.77% were reached within
520 24 h for GC and GCB, respectively. The low release rate from GCB may be attributed to
521 denser gel matrix and enhanced structural network crosslinking via intra/intermolecular
522 hydrogen bonding related to the incorporation of fibrillar BC. By comparing the release rates
523 of prepared gel scaffolds, GC showed increasing rapid release reaching more than 90%
524 cumulative release after 96 h. This rapid release process was attributed to the high
525 hydrophilicity of the gel causing the matrix to significantly swell and eventually disintegrate
526 [39]. On the other hand, GCB gel scaffold approached equilibrium released after 72 h with
527 maximum release determined as 84.01 ± 3.66% after 168 h. This indicates that the
528 results correlate with the mechanical stability and degradation capacity of the gel in relation
529 to interpenetration with BC. Overall, evaluations performed confirms that sustain release was
530 achieved by incorporating BC in the crosslinked GC gel matrix.

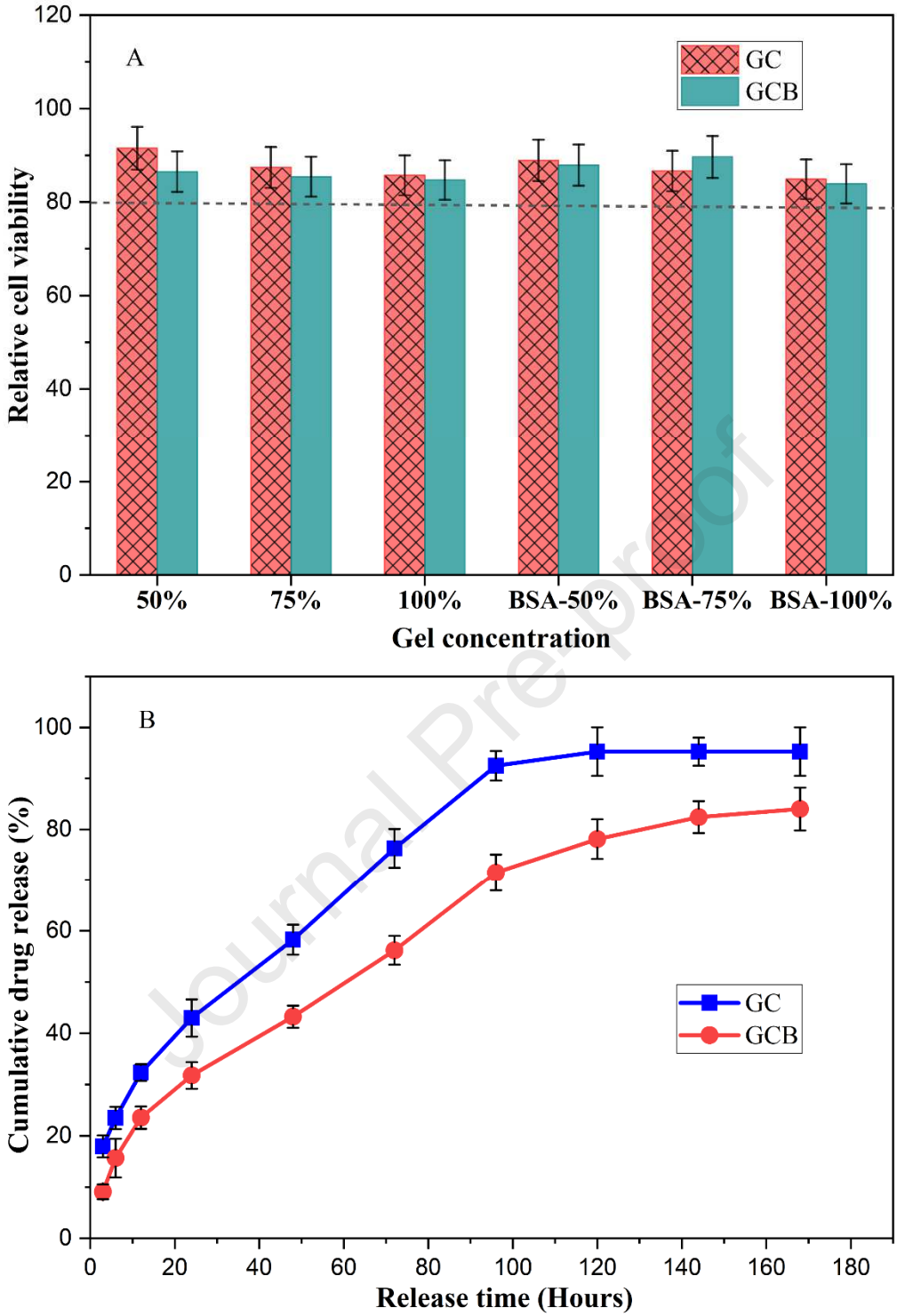

Fig. 8. a) *In vitro* cell cytotoxicity evaluation based on viability of Mouse embryonic fibroblast cells grown on non-loaded GCB (as control) and drug-loaded GCB gel scaffolds at different concentrations in culture medium. Cell seeding concentration at $1x10^5$ cells/mL. b) Cumulative release of BSA from GC and GCB scaffolds at 37 °C in PBS pH 7.4.

The mechanism of BSA release from GC and GCB gel scaffolds was studied by fitting the cumulative drug release data to four different release kinetic equations. The obtained results are displayed in Table 2. By comparing the calculated correlation coefficients (R^2) for

the different release kinetic models, it was observable that in both release medium the release kinetics best fitted with Higuchi's model (R^2 = 0.999 for GC and 0.998 for GCB). This reveals that the release of BSA from GC and GCB matrix based on the square root of time followed a Fickian diffusion process. Further, this phenomenon was supported by Korsmeyer-Peppas model (R^2 = 0.999 for GC and 0.991 for GCB). The n values of GC and GCB were determined as 0.427 and 0.486, respectively, which were <0.5 confirming the release mechanism of BSA predominantly followed Fickian's diffusion [63]. Typically, the release mechanism of Fickian diffusion describes that a substance in the matrix of a porous polymeric material can be released into immersion solution by diffusion via porous channels [64]. Considering BSA is water-insoluble, the hydration of GC and GCB via swelling opened the pore channels of the gel scaffolds thereby facilitating the diffusion of the drug into the release medium.

Table 2
Kinetic assessment of BSA release data from GC and GCB gel scaffolds.

Kinetic models	**Parameters**	**Samples**	
		GC	**GCB**
Zero-order	K_1	0.862	0.708
	R^2	0.963	0.932
First-order	K_1	0.016	0.013
	M_o	78.59	74.35
	R^2	0.988	0.970
Higuchi	K_H	7.764	6.452
	R^2	0.999	0.998
Korsmeyer-Peppas	K_{KP}	11.108	5.441
	n	0.327	0.486
	R^2	0.999	0.982

3.5. Antibacterial activity of gel scaffolds

The antibacterial efficacy of the prepared GCB and drug-loaded GCB gel scaffolds were tested against three different bacteria of *S. aureus*, *E. coli* and *K. pneumonia*. Fig. 9 displays the bacteria resistance results of non-loaded and loaded gel scaffolds. According to observations, the non-loaded (GCB) gel scaffold showed resistance against all tested bacteria strains. This indicates that GCB possessed self-incorporated antibacterial properties. This self-antibacterial may be due to the presence of aldehyde groups in oxidized carrageenan gum. Similar results on antibacterial activity were achieved by Wang et al. in a study that reported the effects oxidized κ-carrageenan gum against *E. coli* and *S. aureus* bacteria [65]. Another study by Zhu et al. investigated and reported the growth inhibition properties of periodate oxidized carrageenan gum against *E. coli*, *S. aureus*, *P. aeruginosa* and *L.*

565 *monocytogenes* bacteria [31]. In accordance with the results obtained from the present study,
566 significant growth inhibition was achieved against *S. aureus* and *E. coli* while samples
567 incubated in *K. pneumonia* medium showed resistance against the bacteria. Based on deduced
568 results, the average growth inhibition zones in *S. aureus* and *E. coli* were determined as 4.1 ±
569 0.20 mm and 2.30 ± 0.62 for GCB as compared to 5.4 ± 0.43 mm and 3.1 ± 0.88 mm for
570 GCB-BSA gel scaffold, respectively.

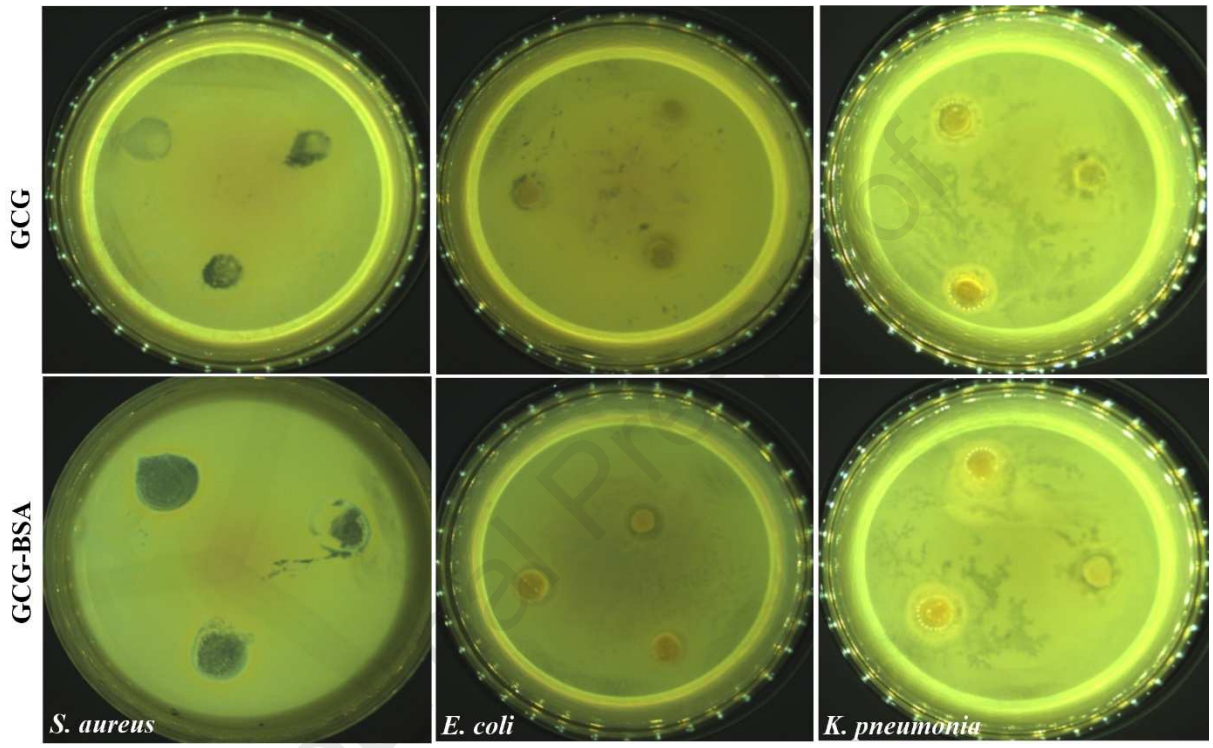

571
572 **Fig. 9.** Antibacterial properties of GCB and GCB-BSA gel scaffolds.

573 ## 4. Conclusions

574 The present study investigates the preparation of injectable self-crosslinked
575 gelatin/aldehyde carrageenan gum gel via the Schiff base nucleophilic reaction followed by
576 interpenetration with bacterial cellulose. Based on results obtained, the prepared gels blended
577 with bacterial cellulose (GCB1, GCB2 and GCB3) exhibited shorter gelation time, higher
578 water uptake and lower *in vitro* degradation as compared to gels without BC (GC1 and GC2).
579 In addition, characterization of the gels by various techniques revealed that the
580 interpenetration of BC in the covalently crosslinked gelatin/aldehyde carrageenan gum
581 network enhanced the tuneable properties. In comparison, GCB gels exhibited higher
582 crystallinity and mechanical stability to GC. Also, GCB showed enhance resistance to shear
583 deformation with variation in temperature and strain as well as possessed good shear thinning

properties. Furthermore, *in vitro* drug release studies demonstrated a sustain release was achieved for GCB samples compared to GC. *In vitro* cytotoxicity assay on the non-loaded and drug loaded GCB gel scaffolds showed significant and high cell viability. Based on bacteria resistance, GCB demonstrated to possess self-antibacterial properties with growth inhibition potency against gram positive and negative bacteria. Overall, the incorporation of BC did not only improve the thermal gelation property of the crosslinked gel matrix, but embedded improve mechanical stability as well as sustain drug release properties compared to gels without BC. Based on good performance in mechanical stability, controlled release and antibacterial activity, we believe that the prepared gel has potential opportunity to be used as an injectable drug delivery system for wound healing and tissue regeneration applications.

Author contributions:

This study conceptualization and methodology was performed by Fahanwi Asabuwa Ngwabebhoh. Formal analysis was done by Fahanwi Asabuwa Ngwabebhoh, Rahul Patwa and Oyunchimeg Zandraa. Investigation and data curation were carried out by Fahanwi Asabuwa Ngwabebhoh, Rahul Patwa and Oyunchimeg Zandraa. Writing-original draft preparation was done by Fahanwi Asabuwa Ngwabebhoh. The paper was reviewed, edited and supervised by Nabanita Saha and Petr Saha.

Declaration of Competing Interest

The authors declare no conflict of interest.

Acknowledgements

The authors acknowledge the support of this work by Tomas Bata University in Zlin and the Ministry of Education, Youth & Sports of the Czech Republic - DKRVO (RP/CPS/2020/005).

References

[1] J. Li, X. Xu, Z. Chen, T. Wang, Z. Lu, W. Hu, L. Wang, Zein/gum Arabic nanoparticle-stabilized Pickering emulsion with thymol as an antibacterial delivery system, Carbohydrate Polymers 200 (2018) 416-426.

[2] B.A. Khan, A. Khan, M.K. Khan, V.A. Braga, Preparation and properties of High sheared Poly(Vinyl Alcohol)/Chitosan blended Hydrogels films with Lawsonia inermis extract as wound dressing, Journal of Drug Delivery Science and Technology (2020) 102227.

[3] T. Maver, S. Hribernik, T. Mohan, D.M. Smrke, U. Maver, K. Stana-Kleinschek, Functional wound dressing materials with highly tunable drug release properties, RSC Advances 5(95) (2015) 77873-77884.

[4] J. Qu, X. Zhao, Y. Liang, T. Zhang, P.X. Ma, B. Guo, Antibacterial adhesive injectable hydrogels with rapid self-healing, extensibility and compressibility as wound dressing for joints skin wound healing, Biomaterials 183 (2018) 185-199.

[5] B.A. Khan, S. Ullah, M.K. Khan, B. Uzair, F. Menaa, V.A. Braga, Fabrication, Physical Characterizations, and In Vitro, In Vivo Evaluation of Ginger Extract-Loaded Gelatin/Poly(Vinyl Alcohol) Hydrogel Films Against Burn Wound Healing in Animal Model, AAPS PharmSciTech 21(8) (2020) 323.

[6] M. Fan, Y. Ma, H. Tan, Y. Jia, S. Zou, S. Guo, M. Zhao, H. Huang, Z. Ling, Y. Chen, X. Hu, Covalent and injectable chitosan-chondroitin sulfate hydrogels embedded with chitosan microspheres for drug delivery and tissue engineering, Materials Science and Engineering: C 71 (2017) 67-74.

[7] D.R. Griffin, W.M. Weaver, P.O. Scumpia, D. Di Carlo, T. Segura, Accelerated wound healing by injectable microporous gel scaffolds assembled from annealed building blocks, Nature Materials 14(7) (2015) 737-744.

[8] N.Q. Tran, Y.K. Joung, E. Lih, K.D. Park, In situ forming and rutin-releasing chitosan hydrogels as injectable dressings for dermal wound healing, Biomacromolecules 12(8) (2011) 2872-2880.

[9] B. Balakrishnan, M. Mohanty, P.R. Umashankar, A. Jayakrishnan, Evaluation of an in situ forming hydrogel wound dressing based on oxidized alginate and gelatin, Biomaterials 26(32) (2005) 6335-6342.

[10] Y. Dong, M. Rodrigues, X. Li, S.H. Kwon, N. Kosaric, S. Khong, Y. Gao, W. Wang, G.C. Gurtner, Injectable and tunable gelatin hydrogels enhance stem cell retention and improve cutaneous wound healing, Advanced Functional Materials 27(24) (2017) 1606619.

[11] D. Loessner, C. Meinert, E. Kaemmerer, L.C. Martine, K. Yue, P.A. Levett, T.J. Klein, F.P. Melchels, A. Khademhosseini, D.W. Hutmacher, Functionalization, preparation and use of cell-laden gelatin methacryloyl–based hydrogels as modular tissue culture platforms, Nature Protocols 11(4) (2016) 727.

[12] X.Q. Sun, C. Ma, W.L. Gong, Y.N. Ma, Y.H. Ding, L. Liu, Biological properties of sulfanilamide-loaded alginate hydrogel fibers based on ionic and chemical crosslinking for wound dressings, International Journal of Biological Macromolecules 157 (2020) 522-529.

[13] W.H. Chang, Y. Chang, P.H. Lai, H.W. Sung, A genipin-crosslinked gelatin membrane as wound-dressing material: in vitro and in vivo studies, Journal of Biomaterials Science-Polymer Edition 14(5) (2003) 481-495.

[14] N. Gull, S.M. Khan, O.M. Butt, A. Islam, A. Shah, S. Jabeen, S.U. Khan, A. Khan, R.U. Khan, M.T.Z. Butt, Inflammation targeted chitosan-based hydrogel for controlled release of diclofenac sodium, International Journal of Biological Macromolecules 162 (2020) 175-187.

[15] K.A. Kristiansen, A. Potthast, B.E. Christensen, Periodate oxidation of polysaccharides for modification of chemical and physical properties, Carbohydrate Research 345(10) (2010) 1264-1271.

[16] E. Shumilina, Y.A. Shchipunov, Chitosan–carrageenan gels, Colloid Journal 64(3) (2002) 372-378.

[17] A. Dafe, H. Etemadi, H. Zarredar, G.R. Mahdavinia, Development of novel carboxymethyl cellulose/k-carrageenan blends as an enteric delivery vehicle for probiotic bacteria, International Journal of Biological Macromolecules 97 (2017) 299-307.

[18] J.S. Varghese, N. Chellappa, N.N. Fathima, Gelatin–carrageenan hydrogels: Role of pore size distribution on drug delivery process, Colloids and Surfaces B: Biointerfaces 113 (2014) 346-351.

[19] J. Guo, L. Ge, X. Li, C. Mu, D. Li, Periodate oxidation of xanthan gum and its crosslinking effects on gelatin-based edible films, Food Hydrocolloids 39 (2014) 243-250.

[20] A.R.G. Dias, E. da Rosa Zavareze, E. Helbig, F.A. de Moura, C.G. Vargas, C.F. Ciacco, Oxidation of fermented cassava starch using hydrogen peroxide, Carbohydrate Polymers 86(1) (2011) 185-191.

[21] F. Wahid, X.-H. Hu, L.-Q. Chu, S.-R. Jia, Y.-Y. Xie, C. Zhong, Development of bacterial cellulose/chitosan based semi-interpenetrating hydrogels with improved mechanical and antibacterial properties, International Journal of Biological Macromolecules 122 (2019) 380-387.

[22] F.A. Ngwabebhoh, O. Zandraa, R. Patwa, N. Saha, Z. Capáková, P. Saha, Self-crosslinked chitosan/dialdehyde xanthan gum blended hypromellose hydrogel for the controlled delivery of ampicillin, minocycline and rifampicin, International Journal of Biological Macromolecules (2020).

[23] S. Hamedi, S.A. Shojaosadati, V. Najafi, V. Alizadeh, A novel double-network antibacterial hydrogel based on aminated bacterial cellulose and schizophyllan, Carbohydrate Polymers 229 (2020) 115383.

[24] F.A. Ngwabebhoh, U. Yildiz, Nature□derived fibrous nanomaterial toward biomedicine and environmental remediation: Today's state and future prospects, Journal of Applied Polymer Science 136(35) (2019) 47878.

[25] Y. Li, H. Jiang, W. Zheng, N. Gong, L. Chen, X. Jiang, G. Yang, Bacterial cellulose–hyaluronan nanocomposite biomaterials as wound dressings for severe skin injury repair, Journal of Materials Chemistry B 3(17) (2015) 3498-3507.

[26] I. Sulaeva, H. Hettegger, A. Bergen, C. Rohrer, M. Kostic, J. Konnerth, T. Rosenau, A. Potthast, Fabrication of bacterial cellulose-based wound dressings with improved performance by impregnation with alginate, Materials Science and Engineering: C 110 (2020) 110619.

[27] A. Svensson, E. Nicklasson, T. Harrah, B. Panilaitis, D.L. Kaplan, M. Brittberg, P. Gatenholm, Bacterial cellulose as a potential scaffold for tissue engineering of cartilage, Biomaterials 26(4) (2005) 419-431.

[28] H. Yan, D. Huang, X. Chen, H. Liu, Y. Feng, Z. Zhao, Z. Dai, X. Zhang, Q. Lin, A novel and homogeneous scaffold material: preparation and evaluation of alginate/bacterial cellulose nanocrystals/collagen composite hydrogel for tissue engineering, Polymer Bulletin 75(3) (2018) 985-1000.

[29] W. Li, B. Wang, M. Zhang, Z. Wu, J. Wei, Y. Jiang, N. Sheng, Q. Liang, D. Zhang, S. Chen, All-natural injectable hydrogel with self-healing and antibacterial properties for wound dressing, Cellulose 27(5) (2020) 2637-2650.

[30] S. Bandyopadhyay, N. Saha, P. Saha, Characterization of Bacterial Cellulose Produced using Media Containing Waste Apple Juice, Appl. Biochem. Microbiol. 54(6) (2018) 649-657.

[31] M. Zhu, L. Ge, Y. Lyu, Y. Zi, X. Li, D. Li, C. Mu, Preparation, characterization and antibacterial activity of oxidized kappa-carrageenan, Carbohydrate Polymers 174 (2017) 1051-1058.

[32] P. Muangman, S. Opasanon, S. Suwanchot, O. Thangthed, Efficiency of microbial cellulose dressing in partial-thickness burn wounds, The Journal of the American College of Certified Wound Specialists 3(1) (2011) 16-19.

[33] Y. Lu, X. Zhao, S. Fang, Characterization, antimicrobial properties and coatings application of gellan gum oxidized with hydrogen peroxide, Foods 8(1) (2019) 31.

[34] V. Kumar, T. Yang, HNO3/H3PO4–NANO2 mediated oxidation of cellulose — preparation and characterization of bioabsorbable oxidized celluloses in high yields and with different levels of oxidation, Carbohydrate Polymers 48(4) (2002) 403-412.

[35] F. Ganji, M.J. Abdekhodaie, A. Ramazani S.A, Gelation time and degradation rate of chitosan-based injectable hydrogel, Journal of Sol-Gel Science and Technology 42(1) (2007) 47-53.

[36] D. Gupta, C.H. Tator, M.S. Shoichet, Fast-gelling injectable blend of hyaluronan and methylcellulose for intrathecal, localized delivery to the injured spinal cord, Biomaterials 27(11) (2006) 2370-2379.

[37] S.I. Erdagi, F.A. Ngwabebhoh, U. Yildiz, Genipin crosslinked gelatin-diosgenin-nanocellulose hydrogels for potential wound dressing and healing applications, International Journal of Biological Macromolecules 149 (2020) 651-663.

[38] L.-Y. Wang, G.-H. Ma, Z.-G. Su, Preparation of uniform sized chitosan microspheres by membrane emulsification technique and application as a carrier of protein drug, Journal of Controlled Release 106(1) (2005) 62-75.

[39] J. Siepmann, N.A. Peppas, Modeling of drug release from delivery systems based on hydroxypropyl methylcellulose (HPMC), Advanced Drug Delivery Reviews 64 (2012) 163-174.

[40] Y. Ren, X. Zhao, X. Liang, P.X. Ma, B. Guo, Injectable hydrogel based on quaternized chitosan, gelatin and dopamine as localized drug delivery system to treat Parkinson's disease, International Journal of Biological Macromolecules 105 (2017) 1079-1087.

[41] R.W. Korsmeyer, R. Gurny, E. Doelker, P. Buri, N.A. Peppas, Mechanisms of solute release from porous hydrophilic polymers, International Journal of Pharmaceutics 15(1) (1983) 25-35.

[42] Y. Gao, J. Zuo, N. Bou-Chacra, T.d.J.A. Pinto, S.-D. Clas, R.B. Walker, R. Löbenberg, In vitro release kinetics of antituberculosis drugs from nanoparticles assessed using a modified dissolution apparatus, Biomed Res. Int. 2013 (2013) 136590-136590.

[43] X. Ma, T. Xu, W. Chen, H. Qin, B. Chi, Z. Ye, Injectable hydrogels based on the hyaluronic acid and poly (γ-glutamic acid) for controlled protein delivery, Carbohydrate Polymers 179 (2018) 100-109.

[44] M. Pooresmaeil, H. Namazi, Facile preparation of pH-sensitive chitosan microspheres for delivery of curcumin; characterization, drug release kinetics and evaluation of anticancer activity, International Journal of Biological Macromolecules 162 (2020) 501-511.

[45] Y. Zhou, Y. Ye, W. Zhang, S. Li, J. Chen, S. Wang, D. Li, C. Mu, Oxidized amylose with high carboxyl content: A promising solubilizer and carrier of linalool for antimicrobial activity, Carbohydrate Polymers 154 (2016) 13-19.

[46] S. Pietrzyk, L. Juszczak, T. Fortuna, M. Łabanowska, E. Bidzińska, K. Błoniarczyk, The influence of Cu (II) ions on physicochemical properties of potato starch oxidised by hydrogen peroxide, Starch□Stärke 64(4) (2012) 272-280.

[47] L. Zhang, J. Liu, X. Zheng, A. Zhang, X. Zhang, K. Tang, Pullulan dialdehyde crosslinked gelatin hydrogels with high strength for biomedical applications, Carbohydrate Polymers 216 (2019) 45-53.

[48] N. Annabi, A. Fathi, S.M. Mithieux, P. Martens, A.S. Weiss, F. Dehghani, The effect of elastin on chondrocyte adhesion and proliferation on poly (ε-caprolactone)/elastin composites, Biomaterials 32(6) (2011) 1517-1525.

[49] M.-x. Tang, Y.-c. Lei, Y. Wang, D. Li, L.-j. Wang, Rheological and structural properties of sodium caseinate as influenced by locust bean gum and κ-carrageenan, Food Hydrocolloids (2020) 106251.

[50] P. Paximada, A.A. Koutinas, E. Scholten, I.G. Mandala, Effect of bacterial cellulose addition on physical properties of WPI emulsions. Comparison with common thickeners, Food Hydrocolloids 54 (2016) 245-254.

[51] R. Yegappan, V. Selvaprithiviraj, S. Amirthalingam, R. Jayakumar, Carrageenan based hydrogels for drug delivery, tissue engineering and wound healing, Carbohydrate polymers 198 (2018) 385-400.

[52] L. Gu, T. Li, X. Song, X. Yang, S. Li, L. Chen, P. Liu, X. Gong, C. Chen, L. Sun, Preparation and characterization of methacrylated gelatin/bacterial cellulose composite hydrogels for cartilage tissue engineering, Regenerative Biomaterials 7(2) (2019) 195-202.

[53] J. Yu, P.R. Chang, X. Ma, The preparation and properties of dialdehyde starch and thermoplastic dialdehyde starch, Carbohydrate Polymers 79(2) (2010) 296-300.

[54] S. Ye, L. Jiang, C. Su, Z. Zhu, Y. Wen, W. Shao, Development of gelatin/bacterial cellulose composite sponges as potential natural wound dressings, International Journal of Biological Macromolecules 133 (2019) 148-155.

[55] D. Tahtat, M. Mahlous, S. Benamer, A.N. Khodja, H. Oussedik-Oumehdi, F. Laraba-Djebari, Oral delivery of insulin from alginate/chitosan crosslinked by glutaraldehyde, International Journal of Biological Macromolecules 58 (2013) 160-168.

[56] M. Khamrai, S.L. Banerjee, P.P. Kundu, Modified bacterial cellulose based self-healable polyeloctrolyte film for wound dressing application, Carbohydrate Polymers 174 (2017) 580-590.

[57] C. Peña, K. De La Caba, A. Eceiza, R. Ruseckaite, I. Mondragon, Enhancing water repellence and mechanical properties of gelatin films by tannin addition, Bioresource technology 101(17) (2010) 6836-6842.

[58] A. Bigi, S. Panzavolta, K. Rubini, Relationship between triple-helix content and mechanical properties of gelatin films, Biomaterials 25(25) (2004) 5675-5680.

[59] C. Asma, E. Meriem, B. Mahmoud, B. Djaafer, Physicochemical characterization of gelatin-cmc composite edibles films from polyion-complex hydrogels, Journal of the Chilean Chemical Society 59(1) (2014) 2279-2283.

795 [60] S. Taokaew, S. Seetabhawang, P. Siripong, M. Phisalaphong, Biosynthesis and
796 characterization of nanocellulose-gelatin films, Materials 6(3) (2013) 782-794.

797 [61] W. Treesuppharat, P. Rojanapanthu, C. Siangsanoh, H. Manuspiya, S. Ummartyotin,
798 Synthesis and characterization of bacterial cellulose and gelatin-based hydrogel
799 composites for drug-delivery systems, Biotechnology Reports 15 (2017) 84-91.

800 [62] S. Kiortsis, K. Kachrimanis, T. Broussali, S. Malamataris, Drug release from tableted
801 wet granulations comprising cellulosic (HPMC or HPC) and hydrophobic component,
802 European Journal of Pharmaceutics and Biopharmaceutics 59(1) (2005) 73-83.

803 [63] M.A. da Silva, A.C.K. Bierhalz, T.G. Kieckbusch, technology, Modelling natamycin
804 release from alginate/chitosan active films, International Journal of Food Science 47(4)
805 (2012) 740-746.

806 [64] W.-S. Chang, H.-H. Chen, Physical properties of bacterial cellulose composites for
807 wound dressings, Food Hydrocolloids 53 (2016) 75-83.

808 [65] F.F. Wang, Z. Yao, H.G. Wu, S.X. Zhang, N.N. Zhu, X. Gai, Antibacterial activities of
809 kappa-carrageenan oligosaccharides, Applied Mechanics and Materials, Trans Tech
810 Publ, 2012, pp. 194-199.

811

Declaration of interests

☒ The authors declare that they have no known competing financial interests or personal relationships that could have appeared to influence the work reported in this paper.

☐The authors declare the following financial interests/personal relationships which may be considered as potential competing interests:

None